International Journal of Advanced Engineering and Technology Research
ISSN: 3106-8677 (Print), ISSN: 3106-8685 (Online) | Vol. 1, No. 3, 2026

Electric Field-Enhanced Oil Recovery Performance in Shale Inorganic Pores during CO2 Injection: A Molecular-Scale Study

Jieying La

School of Petroleum Engineering, Xi'an Shiyou University, Xi'an 710065, China

Abstract: To solve the problems of strong crude oil adsorption and low displacement efficiency of conventional CO_2 in shale inorganic pores, and to reveal the micro-mechanism of electric field-enhanced CO_2 displacement of shale oil, this paper takes the widely developed quartz inorganic nano-pores in shale as the research object. A quartz-crude oil-CO_2 micro-simulation system was constructed by adopting the method of molecular dynamics simulation combined with theoretical analysis, to systematically study the shale oil displacement effect and micro-interaction characteristics before and after applying electric field. By comparing the relative concentration distribution of crude oil molecules, the radial distribution function (RDF) of CO_2 and crude oil, the wall-oil interaction energy, and the evolution law of molecular motion under the conditions of no electric field (without electric field) and with electric field (with electric field), the influence of electric field on the adsorption-desorption behavior of crude oil and CO_2 displacement efficiency was quantitatively analyzed, and the molecular change characteristics at different time nodes (0.2 ns, 1 ns, 2 ns, 4 ns) were explored. The results show that the application of an external electric field can significantly weaken the adsorption between crude oil molecules and the quartz wall, reduce the interaction energy, promote the miscibility between CO_2 and crude oil, and effectively strip the adsorbed crude oil in the pores; after applying the electric field, the displacement efficiency of quartz inorganic pores increases from 35.92% to 51.96%, with a difference of 9.79%. This paper clarifies the intrinsic mechanism of electric field-enhanced CO_2 oil displacement at the molecular scale, improves the micro-theoretical system of electric field-assisted CO_2 development of shale oil, and provides theoretical basis and technical support for the optimization of electric field synergistic displacement process parameters and on-site technology research and development in shale oil reservoirs.

Keywords: Electric field, Shale Inorganic Pores, Displacement Efficiency.

1. Introduction

With the continuous growth of global energy demand, unconventional oil and gas resources represented by shale oil have become an important strategic replacement for conventional fossil energy. Shale reservoirs are characterized by complex pore structures, ultralow porosity and ultralow permeability, and a large amount of crude oil is confined in nanoscale pore throats in the form of adsorbed oil, resulting in low primary recovery efficiency and restricting the large-scale effective development of shale oil resources [1-3]. Therefore, exploring efficient and environmentally friendly enhanced oil recovery technologies is of great significance for improving shale oil production and resource utilization.

Carbon dioxide flooding is one of the widely applied enhanced oil recovery technologies, which can realize greenhouse gas sequestration while improving oil recovery, presenting remarkable economic and environmental benefits [4]. In shale nanopores, injected CO_2 can displace crude oil through competitive adsorption, miscible mass transfer and interfacial interaction regulation [5,6]. However, limited by the strong adsorption effect between crude oil components and mineral pore walls, conventional CO_2 flooding still faces problems such as insufficient stripping capacity for adsorbed crude oil and limited displacement improvement. It is urgent to develop auxiliary strengthening methods to further optimize the CO_2 displacement effect in shale nano-pore systems [7].

As an efficient physical regulation method, electric field technology can regulate molecular interaction, interfacial adsorption characteristics and fluid miscibility at the microscopic scale, and has broad application potential in the field of unconventional oil and gas exploitation [8-10]. Existing studies have confirmed that an external electric field can change the adsorption–desorption behavior of organic molecules on mineral surfaces, adjust the interaction force between fluid molecules, and break the stable adsorption state of crude oil on pore walls [11-16]. Nevertheless, most current researches focus on macroscopic displacement experiments, and there are few systematic studies on the microscopic mechanism of electric field assisting CO_2 to displace shale oil. The microscopic regulation law of an electric field on crude oil distribution, adsorption state and CO_2 miscibility in shale inorganic nanopores still remains unclear, which restricts the further popularization and application of electric field synergistic CO_2 flooding technology [17-19].

Inorganic pores dominated by quartz are widely developed in shale reservoirs, which are key storage spaces for shale oil. The microscopic adsorption mechanism of crude oil in quartz pores and the response characteristics to an external electric field are essential to reveal the multi-field synergistic displacement mechanism. Molecular dynamics simulation can intuitively reflect the molecular distribution, interfacial interaction and dynamic evolution law of fluid in nano-confined spaces, and has become an effective means to explore the microscopic mechanism of shale oil displacement.

In view of this, this study takes typical quartz inorganic nanopores as the research object, constructs a quartz–crude oil–CO_2 microscopic simulation system, and adopts molecular dynamics simulation combined with theoretical

analysis to carry out research. By analyzing the crude oil concentration distribution, adsorption layer evolution, interaction energy variation and radial distribution function characteristics before and after electric field application, the influence of an electric field on shale oil adsorption–desorption behavior and CO_2 displacement efficiency is quantitatively clarified. Furthermore, the intrinsic mechanism of the electric field strengthening CO_2 displacement is revealed from the perspective of competitive adsorption and fluid mutual solubility. The research results are expected to supplement the microscopic theoretical research of electric field-assisted CO_2 shale oil recovery, and provide theoretical reference and technical support for the parameter optimization and field application of electric field synergistic flooding technology in shale reservoirs.

2. Simulation Method

2.1. Molecular Structure

The Shale reservoirs contain organic and inorganic substances. Organic matter in shale reservoirs is generally accompanied by abundant inorganic minerals. In the early hydrocarbon generation stage, shale oil is mainly adsorbed in organic pores. With the enhancement of hydrocarbon generation capacity, the yield of shale oil increases, and oil molecules gradually migrate to adjacent pore spaces. Consequently, a large amount of free shale oil occurs in inorganic pores [20]. In addition, relevant studies have proven that clay minerals possess strong adsorption capacity for shale with low organic matter content. The existence of inorganic pores significantly affects the occurrence state and migration behavior of shale oil in nanopores. Especially for shale oil reservoirs with developed pore spaces, inorganic pores play a vital role in the overall oil displacement and recovery process. Inorganic pore walls generally exhibit strong hydrophilicity. The mineral composition of the shale sample in this study includes quartz, feldspar, pyrite and clay minerals. Therefore, to accurately clarify the replacement mechanism of CO_2 in shale inorganic pores, a molecular dynamics model of quartz inorganic pore walls was constructed.

Quartz is widely used to establish inorganic pore walls in molecular simulation of shale systems. In this paper, the quartz unit cell was cut along the (0 0 1) crystal plane and expanded to construct a supercell for characterizing shale inorganic walls. The quartz surface (Si-O-H) is easily hydroxylated by formation water; thus, fully hydroxylated silica was adopted to represent quartz minerals in the simulation [21]. Silica has two crystal structures: α-SiO_2 and β-SiO_2, among which α-$SiO_2$is widely distributed in shale reservoirs. In this study, the lattice parameters of α-SiO_2were set as follows: a = 0.4913 nm, b = 0.4913 nm, c = 0.5405 nm, with the angles α = 90°, β = 90°, and γ = 120°. During simulation, a stable crystal structure was obtained by cutting the (0 0 1) crystal surface, and hydroxylated quartz surfaces were formed by bonding unconnected oxygen and hydrogen atoms on the pore wall. Finally, the quartz unit cell was expanded to meet the size requirements of the simulation model.

Shale fluid exhibits extremely complex composition. Compositional analysis was conducted to clarify the basic properties of shale oil. The results show that saturated alkanes are the dominant components, with only a small proportion of aromatic hydrocarbons, non-hydrocarbon compounds and asphaltenes. It would be extremely challenging and computationally expensive to establish a simulation model containing all shale oil components. Moreover, it is difficult to formulate a unified component standard for fluids from different shale reservoirs. Accordingly, this study focuses on alkanes, the main constituent of shale oil. To improve simulation efficiency and simplify analysis, shale oil components with similar chemical properties and molecular structures were classified and simplified into three pseudo-components. Three typical alkane molecules, namely $C_{12}H_{26}$, $C_{18}H_{38}$ and $C_{24}H_{50}$, were selected to represent shale oil.

Based on the total component test results of crude oil, the mass fractions of $C_{12}H_{26}$, $C_{18}H_{38}$ and $C_{24}H_{50}$ in the shale oil model without an electric field were set to 46.62%, 18.54% and 34.83%, respectively. In the electric field model, the corresponding mass fractions were 52.76%, 31.47% and 15.77%. Finally, geometric optimization was carried out for oil molecules to achieve structural equilibrium.

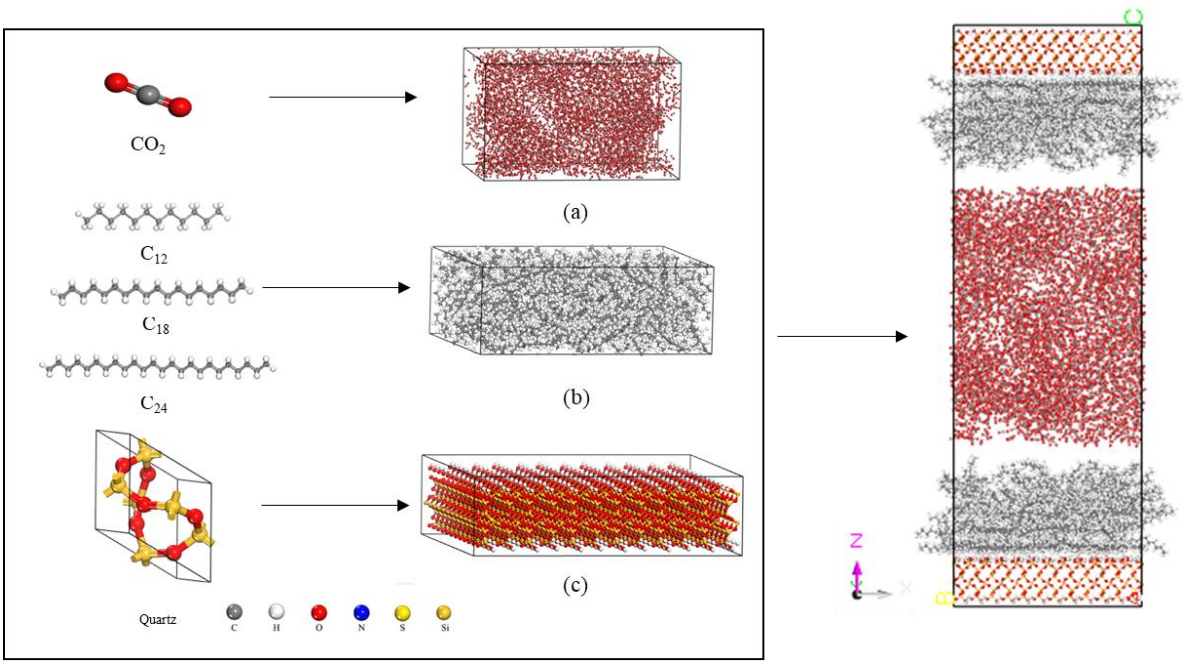

Figure 1. (a) CO_2 box (b) crude oil box (c) Quart box

2.2. Page Numbers

In accordance with the construction procedure of inorganic nanopores, the SiO_2 unit cell was first cut along the (0 0 1) crystal plane and expanded to build a supercell for characterizing shale inorganic pore walls. Since the quartz surface (Si-O-H) is susceptible to hydroxylation by formation water, fully hydroxylated SiO_2 was adopted to represent quartz minerals in this study [84]. During the simulation, a stable crystal structure was obtained by cutting the (0 0 1) crystal face of α-SiO_2, and the hydroxylated quartz surface was constructed by bonding unbound oxygen and hydrogen atoms on the pore wall. The quartz unit cell was further expanded to meet the size requirements of this work. As shown in Fig. 1, the quartz mineral model has a surface size of 5.9 × 5.1 nm² and a thickness of 1.1 nm along the z-direction. Except for the surface hydrogen atoms which could rotate via O-H bonds, all pore wall atoms were set as fixed in the simulation [22]. Geometry optimization and molecular dynamics simulation were carried out to optimize the structure and obtain the balanced quartz box model. The cutoff radius was set to 1.25 nm, with the PPPM algorithm for electrostatic forces and the Atom-based algorithm for van der Waals forces. Molecular dynamics simulation was then performed in the NVT ensemble for 1 ns using the Andersen thermostat to achieve the equilibrium configuration of the quartz wall [23, 24].

The Amorphous Cell module was employed to establish the initial crude oil box and CO_2 box separately, followed by geometry optimization to reach structural equilibrium. The Smart algorithm was adopted for geometry optimization with an iteration number of 1×10^4, yielding the balanced configurations of the optimized crude oil and CO_2 boxes (Fig. 1). The optimized crude oil box was relaxed by 1 ns molecular dynamics simulation in the NVT ensemble to acquire its stable structure.

The composite shale oil system, CO_2 system and kerogen pore model were assembled to establish the composite oil-CO_2-wall model, as illustrated in the corresponding figure. Subsequently, the pore walls were fixed, and the COMPASS III [25] force field was assigned to the whole system. The Smart algorithm was used for geometric optimization to minimize the potential energy of all molecules. After that, molecular dynamics simulation was carried out in the NVT ensemble, and the Nosé-Hoover thermostat was utilized to maintain a constant system temperature. The cutoff radius was 1.25 nm [26, 27]; electrostatic interactions were calculated by the PPPM algorithm, and van der Waals interactions were calculated by the Atom-based method. The time step was set to 1 fs, and the total simulation time was 4 ns [28].

3. Literature References

3.1. The Effect of Electric Field on Replacement Efficiency

The Structural differences between organic and inorganic pores in shale oil reservoirs directly govern the adsorption, diffusion, and migration behaviors of molecules following CO_2 injection, thereby determining reservoir development efficiency and carbon sequestration efficacy. Under the scenario of external electric field regulation, clarifying the interaction mechanism between CO_2 and shale oil molecules in inorganic nanopores is crucial for in-depth understanding of the microscopic mechanism underlying electric field-enhanced CO_2 flooding. Molecular dynamics (MD) simulation enables accurate reproduction of microscopic molecular motion processes at the nanoscale, providing a reliable technical approach for investigating the time-dependent evolution rules of molecules in different pore types. Focusing on the reservoir structure of inorganic pores, this section analyzes the molecular variation characteristics during the simulation process. Time-evolution molecular snapshots intuitively exhibit the spatial distribution of molecules in inorganic nanopores at different time points, clearly illustrating the diffusion and adsorption evolution processes of CO_2 molecules within the pores, as well as the changes in the occurrence state, dispersion, and aggregation of shale oil molecules. Meanwhile, combined with molecular distribution characteristics, the dynamic changes in the relative concentration of each component are quantitatively analyzed, which provides microscopic experimental and theoretical support for revealing the influence mechanism of inorganic nanopores on CO_2 injection effects before and after electric field application, and for optimizing reservoir development parameters.

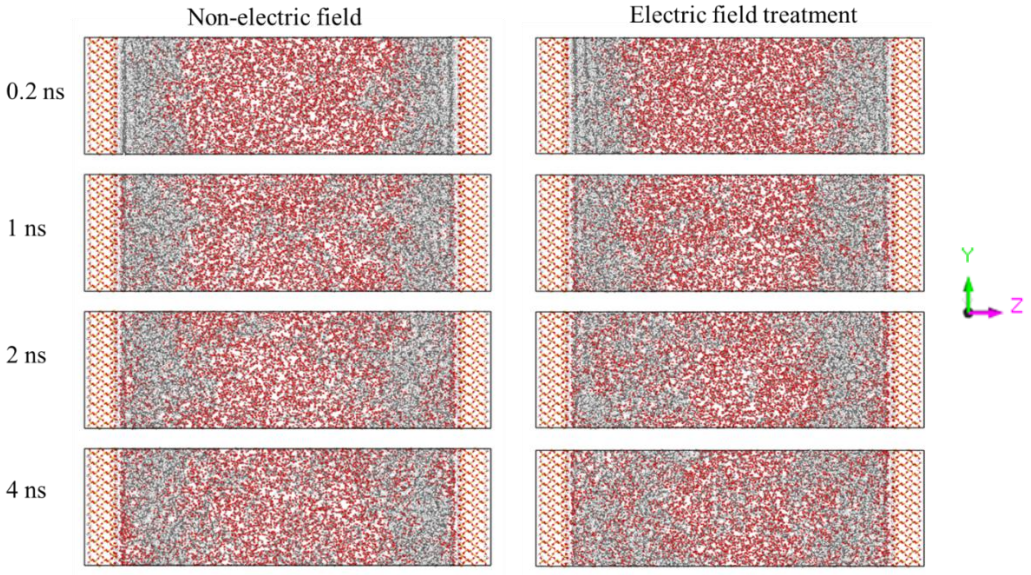

Figure 2. Molecular changes at different time of 0.2 ns, 1 ns, 2 ns and 4 ns

Figure 2 shows the snapshot configurations of the quartz-crude oil-CO_2 system before and after the application of an electric field. From the equilibrium configuration without an electric field, it can be observed that the crude oil components are irregularly distributed along the quartz wall surface, and a small number of oil molecules are free in the pore bulk phase. This distribution is consistent with the initial adsorption state of crude oil molecules on the pore wall, which is consistent with the molecular distribution characteristics of the organic pore system. After CO_2 injection, the crude oil molecules adsorbed on the quartz wall surface are gradually desorbed, and the oil molecules in the bulk phase increase, indicating that CO_2 can effectively displace the adsorbed crude oil.

After the application of an electric field, the distribution of crude oil molecules near the quartz wall surface changes significantly. The adsorption capacity of the quartz wall surface for crude oil is reduced, and the oil molecules adsorbed on the wall surface are further desorbed and converted into the bulk phase. The comparison of the relative concentration of crude oil before and after the application of the electric field shows that the electric field can effectively enhance the desorption of crude oil, reduce the adsorption of crude oil on the pore wall, and improve the displacement efficiency. To clearly compare the difference in oil molecule desorption between different pore types, the relative concentration of crude oil components near the pore wall was statistically analyzed, and the relative concentration data of each component were sorted out.

In order to further clarify the influence of the electric field on the displacement effect, the relative concentration of crude oil components in the system was statistically analyzed. The results show that the electric field can significantly promote the desorption of crude oil molecules adsorbed on the pore wall, reduce the adsorption capacity of the pore wall for crude oil, and increase the content of free oil molecules in the bulk phase, thereby improving the displacement efficiency of CO_2.

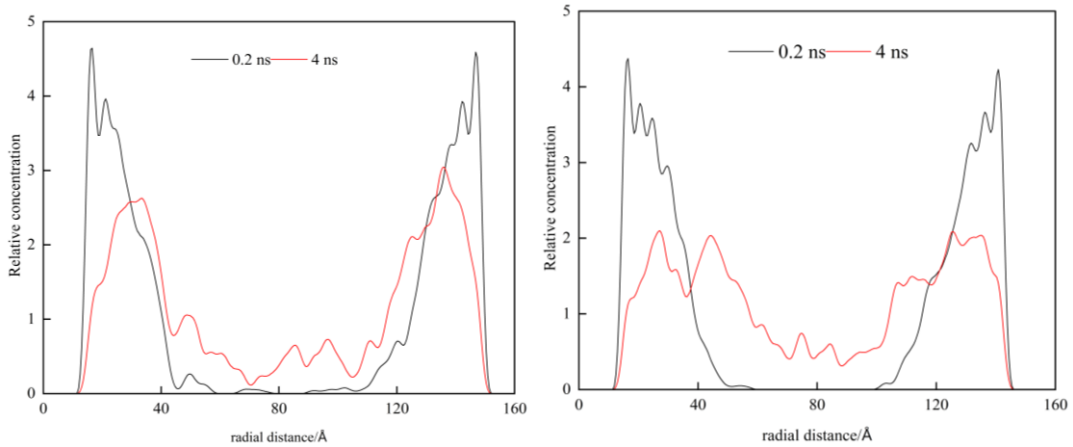

Figure 3. Relative concentration of oil molecules in inorganic pores: before electric field (left), after electric field (right)

Figure 3 presents the relative concentration distribution of shale oil within inorganic pores. It can be observed that distinct peaks emerge near the quartz wall at 0.2 ns, which is attributed to the accumulation of crude oil molecules around the pore wall at the initial stage and the formation of an adsorption layer.

For inorganic pores, as illustrated in Figure 3, without an electric field, the peak values of the adsorption layer on the left side of the quartz wall decrease from 4.64, 3.96 and 3.59 to 1.18, 1.63 and 2.07 respectively, while those on the right side decline from 4.59, 3.92 and 3.35 to 1.52, 2.46 and 2.74. This indicates that CO_2 strips crude oil from the quartz wall surface through competitive adsorption.

After applying an electric field, the peak values of the left adsorption layer drop from 4.37, 3.78 and 3.59 to 1.12, 1.40 and 1.91, and the three peak values of the right adsorption layer reduce from 4.23, 3.67 and 3.26 to 1.41, 1.97 and 2.00 correspondingly.

Table 1. Displacement Efficiency

Displacement Efficiency/%	Inorganic Pores (Quartz)
Non-electric field	42.17%
Electric field treatment	51.96%
Difference	9.79%

The total number of molecules in the model system remains constant. The relative concentration of the adsorption layer decreases while that of the bulk phase increases, indicating that crude oil molecules originally distributed in the adsorbed phase gradually migrate toward the bulk phase. To accurately analyze the effect of an electric field on shale oil recovery efficiency, the displacement efficiency of shale oil is calculated based on the relative concentration of shale oil in inorganic nanopores.

By comparing the difference in the relative concentration distribution of shale oil in organic and inorganic nanopores between the initial state (T=0.2 ns) and the equilibrium state (T=4.0 ns), the influence of CO_2 on shale oil displacement efficiency before and after electric field application is quantified. As shown in Table 1, the displacement efficiency of shale oil in inorganic pores is 42.17% without an electric field. After applying an electric field to crude oil, the displacement efficiencies of inorganic pores are 51.96%. Compared with the condition without an electric field, the maximum displacement efficiency of inorganic pores increases by 9.79% under the electric field.

3.2. The Effect of Electric Field on CO_2-Enhanced Oil Recovery in Shale Inorganic Nanopores

This study adopts electric field technology to explore its influence on shale oil recovery efficiency during CO_2 injection. After CO_2 is injected into shale nanopores, part of the CO_2 molecules are adsorbed near the pore walls and strip crude oil from the pore surfaces via competitive adsorption. The remaining CO_2 molecules are far from the pore walls with weak wall interactions, dissolve in crude oil, and improve the flow and diffusion capacity of crude oil.

Interaction energy refers to the energy released or absorbed by the entire system when a molecule or atom is adsorbed onto a solid surface, serving as a direct indicator to quantify the interaction strength between adsorbents and adsorbates. Generally, adsorption is an exothermic process, and the adsorption energy is expressed as a negative value. A larger absolute value indicates stronger bonding between adsorbates and solid surfaces, as well as higher stability of the formed adsorption system.

Accordingly, the interaction energy between CO_2 and crude oil components is adopted to characterize the positive driving force for crude oil stripping by CO_2. A stronger CO_2-crude oil interaction energy corresponds to a greater positive driving force, demonstrating that CO_2 can more easily detach crude oil components from pore walls. The interaction energy between crude oil components and pore walls represents the resistance encountered during CO_2-induced crude oil stripping. Stronger interaction energy between crude oil components and pore walls means crude oil is more readily adsorbed on pore surfaces, leading to higher resistance for CO_2 to strip adsorbed crude oil and making crude oil detachment more difficult.

Therefore, the difference in interaction energy between CO_2-wall and crude oil-wall, namely the difference between positive driving force and resistance, is used in this study to evaluate the difficulty of CO_2 stripping crude oil components from pore walls. A larger energy difference indicates that CO_2 can more effectively remove crude oil components on pore walls, while a smaller energy difference suggests that crude oil stripping by CO_2 becomes more difficult.

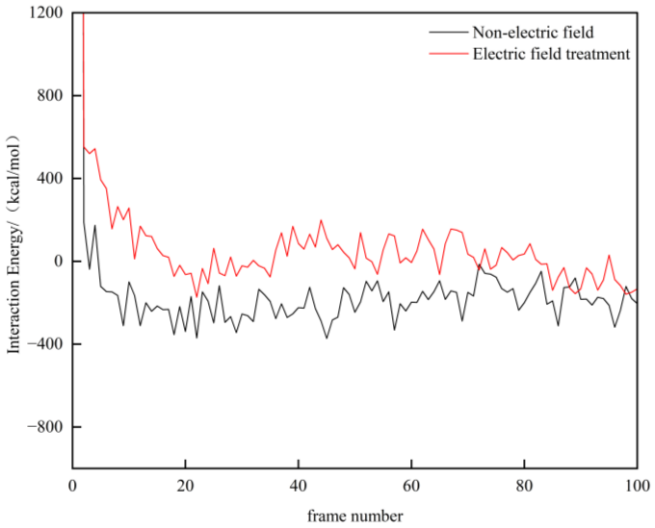

Figure 4. Variation of Wall-oil Interaction Energy Before and After Electric Field Application

Figure 4 shows the variation of interaction energy in inorganic pores before and after electric field application. It can be seen that the absolute value of the interaction energy between CO_2 and crude oil components is consistently higher than that between crude oil components and the pore wall, which indicates that CO_2 can overcome the resistance and strip crude oil from the pore wall.

After an electric field is applied to crude oil, the interaction energy between CO_2 and crude oil increases gradually, suggesting a continuous rise in the positive driving force and an enhanced capacity of CO_2 to strip different crude oil components from the pore wall. Meanwhile, the interaction energy between crude oil and the pore wall decreases progressively, which means the adsorption effect of the pore wall on crude oil components is weakened, and the resistance hindering the detachment of crude oil from the wall is reduced.

Table 2. Interaction Energy

	Non-electric field (kcal/mol)	Electric field treatment (kcal/mol)
CO_2-oil	-10698.4598	-10769.29196
oil-wall	-167.50	-2.20
difference	-10530.96	-10767.09

The average value of the stabilized interaction energy was calculated as the final interaction energy of the model. Table 2 presents the interaction energy results of the pore wall, crude oil components and CO_2 system before and after electric field application.

As listed in the table, the interaction energy differences in inorganic pores without and with the electric field are -10530.96 kcal/mol and -10767.09 kcal/mol, respectively. This reveals that the difference in interaction energy between CO_2-crude oil components and crude oil components-pore wall in inorganic pores gradually increases after the electric field is applied. It demonstrates that the electric field facilitates the stripping of crude oil components from inorganic pore walls by CO_2.

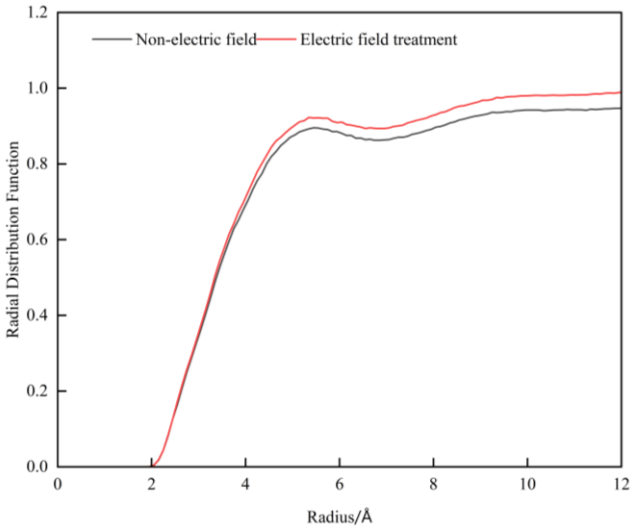

Figure 5. Radial distribution function of CO_2 and crude oil

By calculating and analyzing the radial distribution function g(r) between CO_2 and crude oil before and after electric field application, the influence of the electric field on the mutual solubility characteristics of CO_2 and crude oil can be clarified. The radial distribution function g(r) characterizes the spatial distribution probability of fluid molecules at a given position. A higher g(r) value indicates a higher aggregation degree and stronger interaction between CO_2 and crude oil molecules, corresponding to better mutual solubility of the system.

As shown in Figure 5 in the inorganic pore structure, the first main peak value of the radial distribution function between CO_2 and crude oil is 0.93 under the electric field, while the corresponding peak value is 0.90 without the electric field. The comparison shows that the peak values of the radial distribution function between CO_2 and crude oil under the electric field are higher than those in the electric-field-free condition. This indicates that an external electric field can effectively enhance the interaction strength between CO_2 and crude oil and improve their mutual miscibility.

4. Summary

This chapter investigates the influence of an electric field on shale oil displacement efficiency and its enhancement mechanism, with a focus on inorganic quartz pores. Combining molecular simulation with theoretical analysis, the regulation effect and intrinsic mechanism of the electric field are explored, aiming to provide theoretical and simulation support for electric field-enhanced shale oil recovery technology. A quartz–crude oil–CO_2 simulation system is constructed, and the model is optimized by means of the polymer-consistent force field and molecular dynamics method. Based on snapshot configuration observation, concentration analysis, interaction energy calculation and radial distribution function analysis, together with theoretical discussion, the adsorption–desorption behavior, displacement efficiency variation and microscopic mechanism of shale oil under an electric field are systematically revealed.

Molecular simulation results demonstrate that the electric field can significantly alter the distribution and adsorption characteristics of shale oil in inorganic pores. In the absence of an electric field, crude oil molecules accumulate along pore walls to form dense adsorption layers, with a low content of bulk crude oil. The injection of CO_2 can strip partial crude oil from pore surfaces, and such stripping effect is greatly strengthened after electric field application. The adsorption capacity of crude oil on pore walls declines while the bulk-phase oil content increases, which verifies that the electric field weakens the adsorption interaction between crude oil and pore walls and facilitates shale oil desorption. Obvious crude oil concentration peaks appear near pore walls at the initial state; these peaks decline after CO_2 injection and decrease more remarkably with the assistance of an electric field. Without an electric field, the concentration peaks on quartz walls drop from 4.44, 4.11 and 3.56 to 3.32, 2.70 and 2.35, while under the electric field, the corresponding values decrease to 3.45, 2.52 and 1.56, confirming the conversion of crude oil from the adsorbed state to the free state.

In terms of displacement efficiency, the displacement efficiency of inorganic pores is 42.17% without an electric field and increases to 51.96% after electrification, with an increment of 9.79%. The CO_2–crude oil interaction energy acts as the positive driving force for oil stripping, whereas the crude oil–wall interaction energy represents the adsorption resistance. The absolute value of the former is always higher than that of the latter regardless of electric field conditions, proving that CO_2 can effectively remove adsorbed crude oil from quartz walls. The energy difference between the two further expands under the electric field, and the interaction energy difference of inorganic pores reaches −67580.80 kcal/mol after electrification. The electric field enhances the displacement performance by strengthening the stripping capacity of CO_2 and weakening the wall adsorption on crude oil.

Radial distribution function analysis indicates that the electric field improves the mutual miscibility between CO_2 and crude oil. In inorganic pores, the peak value of the radial distribution function between CO_2 and crude oil rises from 0.90 to 0.93 after electric field loading.

This chapter clarifies the regulation law of electric fields on shale oil displacement in inorganic nanopores and illustrates the enhancement mechanism: the electric field strengthens CO_2–crude oil interaction, weakens crude oil–wall adsorption, and improves the mutual solubility of CO_2 and crude oil. The findings deepen the understanding of microscopic displacement mechanisms and provide a theoretical basis for subsequent electric field parameter optimization and the development of efficient shale oil extraction technologies.

References

[1] Boak J, Kleinberg R. Shale gas, tight oil, shale oil and hydraulic fracturing [M]. Future energy. Elsevier, 2020: 67-95.

[2] Yang L I, Qingmin Z, Qi L Y U, et al. Evaluation technology and practice of continental shale oil development in China [J]. Petroleum Exploration and Development, 2022, 49(5): 1098-1109.

[3] Zhang S, Yan J, Hu Q, et al. Integrated NMR and FE-SEM methods for pore structure characterization of Shahejie shale from the Dongying Depression, Bohai Bay Basin [J]. Marine and Petroleum Geology, 2019, 100: 85-94.

[4] Xing L R, Wu Z W, Zhang R Y. Development status and prospect analysis of CCUS industry [J]. International Petroleum Economics, 2021, 29(8): 99-105.

[5] Jia B, Tsau J S, Barati R. A review of the current progress of CO2 injection EOR and carbon storage in shale oil reservoirs [J]. Fuel, 2019, 236: 404-427.

[6] Jia B, Chen Z, Xian C. Investigations of CO2 storage capacity and flow behavior in shale formation [J]. Journal of Petroleum Science and Engineering, 2022, 208: 109659.

[7] Tovar F D, Eide Q, Graue A, et al. Experimental investigation of enhanced recovery in unconventional liquid reservoirs using CO2: a look ahead to the future of unconventional EOR [C]. SPE Unconventional Resources Conference/Gas Technology Symposium. SPE, 2014: D031S007R005.

[8] Rehman M M, Meribout M. Conventional versus electrical enhanced oil recovery: a review [J]. Journal of Petroleum Exploration and Production Technology, 2012, 2(4): 157-167.

[9] Zhang W, Ning Z, Zhang B, et al. Experimental investigation of driving brine water for enhanced oil recovery in tight sandstones by DC voltage [J]. Journal of Petroleum Science and Engineering, 2019, 180: 485-494.

[10] Jia Z, Ning Z, Lyu F, et al. Laboratory evaluation of electrically enhanced oil recovery in tight reservoirs [J]. Energy & Fuels, 2023, 38(1): 200-213.

[11] Guo H, Zhang W, Lu N, et al. CO2 capture on h-BN sheet with high selectivity controlled by external electric field [J]. The Journal of Physical Chemistry C, 2015, 119(12): 6912-6917.

[12] Razmkhah M, Mosavian M T H, Moosavi F, et al. CO2 gas adsorption into graphene oxide framework: Effect of electric and magnetic field [J]. Applied Surface Science, 2018, 456: 318-327.

[13] Sathishkumar N, Wu S Y, Chen H T. Charge-regulated, electric-field and combined effect controlled switchable CO2 capture and separation on penta-C2N nanosheet: A computational study [J]. Chemical Engineering Journal, 2021, 407: 127194.

[14] Xia Y, Cai M, Wang Y, et al. Competitive adsorption mechanisms of multicomponent gases in kaolinite under electric fields: A molecular perspective [J]. Geoenergy Science and Engineering, 2024, 238: 212897.

[15] Wang Y, Liao B, Kong Z, et al. Oscillating electric field effects on adsorption of the methane–water system on kaolinite surface [J]. Energy & Fuels, 2018, 32(11): 11440-11451.

[16] Liao B, Zhang Z, Wang D, et al. External electric field enhances CO2 geological Storage: A molecular dynamics simulation [J]. Applied Surface Science, 2022, 572: 151312.

[17] Zhang W, Ning Z, Cheng Z, et al. Experimental investigation of the role of DC voltage in the wettability alteration in tight sandstones [J]. Langmuir, 2020, 36(40): 11985-11995.

[18] Zhang W, Ning Z, Wang Q, et al. Experimental study on the effects of an electric field on the pore characterization in anode, middle and cathode regions of tight sandstone samples [J]. Geoenergy Science and Engineering, 2023, 223: 211500.

[19] Zhang W, Ning Z, Song L, et al. Unveiling the changes in the molecular groups of tight sandstones in response to an electric Field [J]. ACS omega, 2021, 6(43): 29126-29136.

[20] Xu Y, Lun Z, Pan Z, et al. Occurrence space and state of shale oil: A review [J]. Journal of Petroleum Science and Engineering, 2022, 211: 110183.

[21] Skelton A A, Fenter P, Kubicki J D, et al. Simulations of the quartz (1011)/water interface: a comparison of classical force fields, ab initio molecular dynamics, and X-ray reflectivity experiments [J]. The Journal of Physical Chemistry C, 2011, 115(5): 2076-2088.

[22] Koretsky C M, Sverjensky D A, Sahai N. A model of surface site types on oxide and silicate minerals based on crystal chemistry; implications for site types and densities, multi-site adsorption, surface infrared spectroscopy, and dissolution kinetics [J]. American Journal of Science, 1998, 298(5): 349-438.

[23] Berendsen H J C, Postma J P M, Van Gunsteren W F, et al. Molecular dynamics with coupling to an external bath [J]. The Journal of chemical physics, 1984, 81(8): 3684-3690.

[24] Huang L, Ning Z, Wang Q, et al. Microstructure and adsorption properties of organic matter in Chinese Cambrian gas shale: Experimental characterization, molecular modeling and molecular simulation [J]. International Journal of Coal Geology, 2018, 198: 14-28.

[25] WANG Lu, ZHANG Yifan, LIU Yisheng, et al. Molecular dynamics analysis on occurrence characteristics of shale oil and competitive adsorption mechanism of CO2 and oil [J] Journal of China University of Petroleum (Edition of Natural Science), 2023,47(4):128-13.

[26] Wang S, Javadpour F, Feng Q. Molecular dynamics simulations of oil transport through inorganic nanopores in shale [J]. Fuel, 2016, 171: 74-86.

[27] Bellal A, Assady A. Molecular Simulation of Adsorption and Diffusion Behavior of CO2 in Bakken Nano-Porous Media for Enhanced Oil Recovery Assessment [C]//ARMA US Rock Mechanics/Geomechanics Symposium. ARMA, 2022: ARMA-2022-0336.

[28] Dong X H, Xu W J, Liu H Q, et al. Molecular insight into the oil displacement mechanism of CO2 flooding in the nanopores of shale oil reservoir [J]. Petroleum Science, 2023, 20(6): 3516-3529.